SEPARATION OF TRANSLATIONAL AND ROTATIONAL CONTRIBUTIONS IN SOLUTION STUDIES USING FLUORESCENCE PHOTOBLEACHING RECOVERY

WILLIAM A. WEGENER AND RUDOLF RIGLER
Department of Medical Biophysics, Karolinska Institute, S-104 01 Stockholm 60, Sweden

ABSTRACT   Although fluorescence photobleaching recovery (FPR) experiments are usually interpreted in terms of the translational motions of a fluorescently labeled species, rotational motions can also modulate recovery through the cosine-squared laws for dipolar absorption and emission processes. In a complex interacting system, translational and rotational contributions may both be simultaneously present. We show how these contributions can be separated in solution studies using an FPR setup in which (*a*) the linear polarization of the low-intensity observation beam and the high-intensity photobleaching pulse can be varied independently, and (*b*) all emitted fluorescent photons are counted equally. The fluorescence recovery signal obtained with the observation beam polarized at the magic angle, 54.7°, from the bleach polarization direction is independent of label orientation, whereas the anisotropy function formed from a combination of parallel and perpendicular polarizations isolates the orientational recovery. The anisotropy function is identical to that in fluorescence correlation spectroscopy and, for rigid-body rotational diffusion, can be expressed as a sum of five exponential terms.

INTRODUCTION

The sensitivity and selectivity of fluorescence labels have made them popular for probing the dynamics of complex biological systems. There are two techniques in which the limitations associated with short fluorescence lifetimes (10^{-8} s) have been overcome: fluorescence correlation spectroscopy (FCS) monitors fluctuations, whereas fluorescence photobleaching recovery (FPR) monitors relaxation following an initial photobleaching perturbation. Several groups have considered the effects of rotational diffusion in FCS, but not FPR, experiments for the case of an isolated rigid body that is free in solution. Ehrenberg and Rigler (1974, 1976) showed that the use of 2π collection optics greatly simplifies the rotational expressions. Aragon and Pecora (1975) obtained more complicated FCS expressions assuming restricted right-angle fluorescence detection, but later concluded that collection of fluorescence over 2π or 4π solid angle would be preferable (Aragon and Pecora, 1976). In this communication, we present a theory underlying FPR solution studies, which allows for both rotational and translational contributions.

In the simplest FPR solution studies involving one noninteracting species, rotational and translational contributions are naturally separated because they occur on different time scales. However, if several labeled species are present, or in complex situations involving interacting

Dr. Wegener's present address is Baylor University Medical Research Institute, 3500 Gaston Avenue, Dallas, Texas 75246.

systems, translational relaxation of some components may occur on the same time scale as rotational relaxation of others. FPR experiments may also contain chemical kinetic contributions involving exchange of a label between two differently bleached states. The particular design analyzed below allows one to obtain a recovery signal that is independent of the orientational distribution of fluorescent labels, whereas a combination of measurements can be used to extract orientational information.

Polarization Dependence of Fluorescence Recovery Signal

In our laboratory, FCS and FPR are applied in solution studies to follow motions over arbitrarily long time scales. The setups for these FCS and FPR studies are similar (Rigler et al., 1979; Rigler and Graselli, 1980). In both setups a laser beam is focused on a thin cuvette containing a solution of fluorescently labeled sample. The cuvette is surrounded by a highly reflective paraboloid cavity butted onto a photomultiplier that greatly enhances the efficiency of fluorescence detection by collecting fluorescent photons emitted over 2π solid angle. For FPR work we have recently developed a system in which the laser output is split into two beams. One beam can be turned on and off by an acousto-optic modulator and provides the high-intensity, short-duration bleach pulse. The other beam is greatly attenuated and provides continuous low-level illumination to excite fluorescence and observe recovery. The bleach pulse is linearly polarized vertically, whereas an arbitrarily

directed polarizer can be inserted in the observation beam. The beams are then recombined such that their transverse Gaussian profiles superimpose at the focal region. This split beam arrangement allows us to independently vary the polarizations and intensities of the bleach pulse and the observation beam while maintaining critical alignment of their superimposed focused images on the sample.

Fig. 1 schematically illustrates our design for FPR solution measurements. A small region of fluorescently labeled sample is illuminated by laser light propagating along the y-axis. A brief high-intensity pulse inactivates by irreversible photobleaching a significant fraction of fluorophores and a continuous steady observation beam then stimulates fluorescence from any active fluorophores in the region. We assume the observation beam intensity is sufficiently low to neglect any photobleaching. The bleach and observation profiles are taken to be identical and superimposed through the sample. The bleach pulse is linearly polarized along the vertical z-axis, and the observation beam is linearly polarized in the x-, z-plane along unit vector $\hat{\theta}$ at an angle θ from the z-axis. We assume that all fluorescent photons emanating from the sample were collected equally without bias to their direction of emission or their state of polarization, either by using a focused paraboloid cavity (Ehrenberg and Rigler, 1976) or by other means (Wegener, 1984). The fluorescence signal is assumed to reflect the instantaneous state of the sample. That is, we are primarily interested in dynamics that occur on time scales much longer than fluorescence lifetimes so that any delay between light absorption and reemission can be ignored.

We now derive an expression for the fluorescence signal intensity $F(t)_\theta$ recorded at time t following the end of the bleach pulse using an observation beam polarized at angle θ. We initially assume the sample contains only a single species of fluorescent label whose directional absorption properties are governed by a unique transition dipole fixed in its molecular axes. If $\hat{\mu}$ denotes a unit vector along this absorption dipole, then the angular dependence of the absorption probability is given as $(\hat{\mu} \cdot \hat{\theta})^2$. The relative contribution of an active (photoemitting) label at position r with dipole orientation to the fluorescence signal is $I(r) (\hat{\mu} \cdot \hat{\theta})^2$, where $I(r)$ denotes the intensity of the observation beam at position r. Let $\rho(r, \hat{\mu}, t) \, d^3r d^2\hat{\mu}$ denote the number of active labels with positions within volume element d^3r about r and dipole orientations within $d^2\hat{\mu}$ about $\hat{\mu}$ at time t. Then $F(t)_\theta$ can be expressed as a sum over all positions and 4π orientations according to

$$F(t)_\theta = 3q \iint I(r)(\hat{\mu} \cdot \hat{\theta})^2 \rho(r, \hat{\mu}, t) d^3r d^2\mu, \qquad (1)$$

where q is the product of the label's quantum efficiencies for light absorption, fluorescence emission and detection, and the factor of 3 accounts for the fact that an isotropically averaged value of $(\hat{\mu} \cdot \hat{\theta})^2$ is $1/3$. The distribution is normalized such that integration over all orientations gives the number concentration of active labels $n(r, t)$ at time t at position r, i.e.,

$$n(r, t) = \int \rho(r, \hat{\mu}, t) d^2 \hat{\mu}. \qquad (2)$$

It is easier to work with changes in fluorescence signal, so we define $\Delta F(t)_\theta = F_0 - F(t)_\theta$, where F_0 denotes the signal before bleaching that is θ-independent. If the label concentration before the bleaching pulse is n_0, then F_0 is expressed as

$$F_0 = qn_0 \int I(r) d^3r. \qquad (3)$$

In the case of rotational and translational relaxation with complete recovery of the prebleach level of active labels, $\Delta F(t)_\theta \rightarrow 0$ for any θ as $t \rightarrow \infty$, and $\rho(r, \hat{\mu}, t) \rightarrow n_0/4\pi$.

Because the system was originally randomly oriented, bleaching produces a distribution that is cylindrically symmetric about z. If fluorescence signals differences measured at $\theta = 0°$ and $90°$ are denoted $\Delta F(t)_\parallel$ and $\Delta F(t)_\perp$, respectively, the sum combination $S(t) = \Delta F(t)_\parallel + 2\Delta F(t)_\perp$ can be expressed as

$$S(t) = 3q \int I(r)[n_0 - n(r, t)] d^3r, \qquad (4)$$

which involves only the concentration difference weighted by the beam intensity.

From cylindrical symmetry, we can express the θ-dependence in $\Delta F(t)_\theta$ by expanding $\hat{\theta}$ along axes x and z to
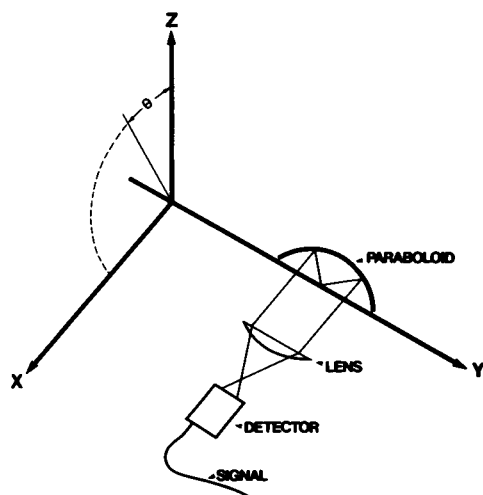

FIGURE 1 A schematic design for solution studies using fluorescence photobleaching recovery is shown. A linearly polarized laser beam directed along the y-axis illuminates a region of fluorescent sample located at the center of a highly reflective paraboloid cavity. Fluorescence emission over 2π is reflected by the parabolic surface, isolated by cutoff filters, and focused by a collection lens through a diaphragm at the front of a gated photomultiplier. The photomultiplier is turned off and the beam power is briefly increased to provide a high-intensity bleach pulse polarized along the z-axis. The power is then greatly reduced to provide a constant observation beam polarized in the x, z-plane at angle θ from the z-axis. The photomultiplier is turned on and the resulting fluorescence signal is recorded.

$$\Delta F(t)_\theta = \cos^2 \theta \, \Delta F(t)_\parallel + \sin^2 \theta \, \Delta F(t)_\perp. \qquad (5)$$

Denoting the fluorescence signal difference measured at $\cos^2 \theta = \frac{1}{3}$ as $\Delta F(t)_m$, Eq. 5 yields

$$\Delta F(t)_m = S(t)/3. \qquad (6)$$

Thus, $\Delta F(t)_\theta$ varies smoothly between extreme values as θ varies from 0° to 90°, and, at the magic angle 54.7°, is independent of the orientational distribution of the label.

Making use of the cylindrical symmetry of $\rho(\mathbf{r}, \hat{\mu}, t)$ about the z-axis, the difference combination $D(t) = \Delta F(t)_\parallel - \Delta F(t)_\perp$ can be expressed as

$$D(t) = -3q \iint I(\mathbf{r}) \, P_2 (\hat{\mu} \cdot \hat{z}) \rho (\mathbf{r}, \hat{\mu}, t) d^3r d^2\hat{\mu}, \qquad (7)$$

where $P_2(\hat{\mu} \cdot \hat{z}) = [3(\hat{\mu} \cdot \hat{z})^2 - 1]/2$ is a second-order Legendre polynomial, and $\hat{z}$ is a unit vector along the z-axis.

Defining the anisotropy function $r(t) = D(t)/S(t)$, Eq. 5 can be rewritten as

$$\Delta F(t)_\theta = \Delta F(t)_m [1 + 2r(t)P_2(\cos \theta)]. \qquad (8)$$

The dependence on observation angle θ is isolated in $P_2(\cos \theta)$, which varies monotonically from 1 at 0°, through 0 at 54.7°, to -0.5 at 90°. The orientationally invariant contribution $\Delta F(t)_m$ provides an overall multiplication factor and is the only term remaining at the magic angle. The magnitude of the changes in signal at different values of θ are completely governed by $r(t)$ as it multiplies $P_2(\cos \theta)$. Hence, the dependence of the fluorescence signal on the orientational distribution of the label resides entirely within the anisotropy function $r(t)$. If the label is distributed isotropically at all positions, then $\rho(\mathbf{r}, \hat{\mu}, t) = n(\mathbf{r}, t)/4\pi$, $\Delta F(t)_\theta$ is independent of θ, and $r(t) = 0$.

Eqs. 5, 6, and 8 express the θ-dependence of the fluorescence signal. Although they were obtained assuming a single fluorescent species, we now show they apply even if the sample contains multiple species. Because fluorescence emission intensities are additive, $F(t)_\theta$ is a sum of terms $F(t)_\theta^i$ for each species i. Assuming $\Delta F(t)_\theta^i$ is given by Eqs. 1 and 3 for each species i, Eqs. 5, 6, and 8 are then reobtained as general relations between measured fluorescence signal quantities. Because $\Delta F(t)_m = \Sigma_i \Delta F(t)_m^i = \frac{1}{3} \Sigma_i S(t)^i$, with $S(t)^i$ given by Eq. 4 for each species i, measurements at the magic angle remain independent of orientational distributions. The measured anisotropy $r(t)$ can be expressed as a weighted sum of contributions $r(t)^i = [\Delta F(t)_\parallel^i - \Delta F(t)_\perp^i]/[\Delta F(t)_\parallel^i + 2\Delta F(t)_\perp^i]$ from each species i according to

$$r(t) = \sum_i \Delta F(t)_m^i r(t)^i / \sum_i \Delta F(t)_m^i. \qquad (9)$$

Thus the relative contribution each species i makes to $r(t)$ involves a fractional weight $[\Delta F(t)_m^i/\Delta F(t)_m]$, which itself is generally time varying.

With these general properties established, we examine the simplest case of solution dynamics involving free diffusion of a single species. We consider a dilute noninteracting solution of identical macromolecules that are labeled in a specific and unique manner by a fluorescent tag. Each particle undergoes Brownian motion and typically moves on the order of its length during the time needed to randomly tumble around. This can be qualitatively shown by evaluating the diffusion coefficients for rotational and translational displacements given by Perrin (1934) for ellipsoids. As such, spatial variation in $I(\mathbf{r})$ or $\rho(\mathbf{r}, \hat{\mu}, t)$ is negligible on this scale and orientational relaxation occurs without involving significant changes in position or coupling to spatial gradients. Likewise, translational relaxation over distances much greater than particle length occur without significant anisotropic effects involving oriented particles. That is, the spatial distribution of the label essentially evolves on a much slower time scale following completion of rotational relaxation near initial positions.

Assuming decoupled translational and rotational relaxation, the conditional probability that an active label with position $\mathbf{r}$ and dipole orientation $\hat{\mu}$ at time t had position $\mathbf{r}'$ and orientation $\hat{\mu}'$ at time 0 factors into the product $W(\mathbf{r}, \mathbf{r}', t) \, \Omega (\hat{\mu}, \hat{\mu}', t)$, where $W(\mathbf{r}, \mathbf{r}', t)$ is the conditional probability that an active label with position $\mathbf{r}$ at time t had position $\mathbf{r}'$ at time 0 and $\Omega(\hat{\mu}, \hat{\mu}', t)$ is the conditional probability that an active label with orientation $\hat{\mu}$ at time t had orientation $\hat{\mu}'$ at time 0. As general properties, $\Omega(\hat{\mu}, \hat{\mu}', t)$ integrates over all $\hat{\mu}$ or $\hat{\mu}'$ at any time t to give unity, equals $\delta(\hat{\mu}, \hat{\mu}')$ at $t = 0$, where δ is the delta function, and, at sufficient time for the completion of rotational relaxation, approaches $1/4\pi$. Likewise, $W(\mathbf{r}, \mathbf{r}', t) = \delta(\mathbf{r}, \mathbf{r}')$ at $t = 0$, and, assuming active labels are neither created nor destroyed after the initial bleach pulse, integrates over all $\mathbf{r}$ or $\mathbf{r}'$ positions at any time t to give unity.

The distribution of active label at time t evolves from the initial distribution as

$$\rho(\mathbf{r}, \hat{\mu}, t) = \iint W(\mathbf{r}, \mathbf{r}', t) \, \Omega (\hat{\mu}, \hat{\mu}', t)$$

$$\cdot \rho (\mathbf{r}', \hat{\mu}', 0) \, d^3r' d^2 \hat{\mu}', \qquad (10a)$$

so the active label concentration $n(\mathbf{r}, t)$ evolves from the initial concentration as

$$n(\mathbf{r}, t) = \int W(\mathbf{r}, \mathbf{r}', t) n(\mathbf{r}', 0) d^3r'. \qquad (10b)$$

Anisotropy Expressions

To obtain a dynamic expression for $r(t)$, we first insert Eq. 10a into Eq. 7. For an unoriented system, $\Omega(\hat{\mu}, \hat{\mu}', t)$ can only depend on the magnitude of the relative angle between $\hat{\mu}$ and $\hat{\mu}'$, and $\Omega(\hat{\mu}, \hat{\mu}', t) = \Omega(\hat{\mu}', \hat{\mu}, t)$. Following Kinosita et al. (1977), this allows us to expand $P_2(\hat{\mu} \cdot \hat{z})$ as $P_2(\hat{\mu} \cdot \hat{\mu}')P_2(\hat{\mu}' \cdot \hat{z})$, plus two other terms. These additional

terms orientationally integrate to zero if the dipole distribution at time t evolved in a cylindrically symmetric fashion from each initial orientation. This condition is ensured if the labels do not move during the bleaching period. Assuming then that the bleach pulse occurs instantaneously at $t = 0$, $r(t)$ can be rearranged and expressed in terms of the expectation value involving the dot product between a label's dipole at times t and 0 as

$$r(t) = r_0 \langle P_2[\hat{\mu}(t) \cdot \hat{\mu}(0)] \rangle. \tag{11}$$

Because $\Omega(\hat{\mu}, \hat{\mu}', t)$ involves only the relative differences between orientations $\hat{\mu}$ and $\hat{\mu}'$, the expectation value can be expressed as

$$\langle P_2[\hat{\mu}(t) \cdot \hat{\mu}(0)] \rangle = \int P_2(\hat{\mu} \cdot \hat{\mu}') \, \Omega\,(\hat{\mu}, \hat{\mu}', t) \mathrm{d}^2\hat{\mu}, \tag{12}$$

for any choice of initial orientation $\hat{\mu}'$.

Using limiting values of $\Omega(\hat{\mu}, \hat{\mu}', t)$, $\langle P_2[\hat{\mu}(t) \cdot \hat{\mu}(0)] \rangle$ is unity at $t = 0$ and vanishes as $t \rightarrow \infty$. The rotational dynamics are completely contained in this term, whereas the r_0 term is a constant discussed in detail later. Because of this separation, dynamic models previously developed elsewhere can be applied here with trivial modifications. For example, the FCS expressions obtained by Ehrenberg and Rigler (1974, 1976) are identified as $0.8\ r\ (t)/r_0$ evaluated for rigid-body rotational diffusion. We also note that the anisotropy function in fluorescence depolarization is identical to $0.4\ r(t)/r_0$ if the emission dipole there is parallel to the absorption dipole (e.g., see Eq. 14 in Kinosita et al., 1977 or Eqs. 20 and 28 in Wahl, 1975).

The most general model we will consider is a label rigidly fixed to a arbitrary particle undergoing rigid-body rotational diffusion. Let D_1, D_2, and D_3 denote the principal rotational diffusion coefficients and μ_1, μ_2, and μ_3 denote components of $\hat{\mu}$ along the associated principal axes that are orthogonal and body fixed. As shown by Ehrenberg and Rigler (1972), $r(t)$ is a sum of five exponentials:

$$r(t) = r_0 \sum_{i=1}^{5} A_i \exp(-E_i t), \tag{13}$$

where

$$A_1 = 3(\mu_2\mu_3)^2 \qquad E_1 = 3(D_s + D_1)$$
$$A_2 = 3(\mu_1\mu_3)^2 \qquad E_2 = 3(D_s + D_2)$$
$$A_3 = 3(\mu_1\mu_2)^2 \qquad E_3 = 3(D_s + D_3)$$
$$A_4 = 3(A + B)/4 \qquad E_4 = 6D_s + 2\Delta$$
$$A_5 = 3(A - B)/4 \qquad E_5 = 6D_s - 2\Delta$$

and

$$D_s = \frac{1}{3}(D_1 + D_2 + D_3);$$

$$\Delta = (D_1^2 + D_2^2 + D_3^2 - D_1D_2 - D_2D_3 - D_3D_1)^{1/2};$$

$$A = \mu_1^4 + \mu_2^4 + \mu_3^4 - \frac{1}{3};$$

$$B = (D_1/\Delta)(\mu_2^4 + \mu_3^4 - 2\mu_1^4 + 2\mu_1^2)$$
$$+ (D_2/\Delta) \cdot (\mu_3^4 + \mu_1^4 - 2\mu_2^4 + 2\mu_2^2)$$
$$+ (D_3/\Delta)(\mu_1^4 + \mu_2^4 - 2\mu_3^4 + 2\mu_3^2) - 2D_s/\Delta,$$

such that the A_i values sum to unity.

If the particle has cylindrical symmetry, these expressions collapse to

$$r(t)/r_0 = 3 \sin^2 \varphi \cos^2 \varphi \mathrm{e}^{-(5D_\perp + D_\parallel)t} + (3/4) \sin^4 \varphi \mathrm{e}^{-(2D_\perp + 4D_\parallel)t}$$
$$+ (1/4)(3 \cos^2 \varphi - 1)^2 \mathrm{e}^{-6D_\perp t}, \tag{14}$$

where $D_\parallel$ and $D_\perp$ denote the diffusion coefficients for rotations about the symmetry axis and a perpendicular to this axis, respectively, and φ denotes the angle that $\hat{\mu}$ makes with the symmetry axis.

Finally, if all three diffusion coefficients are identical and denoted D,

$$r(t) = r_0 \mathrm{e}^{-6Dt}. \tag{15}$$

Assuming that translational relaxation is negligible during the label's rotational relaxation, $r_0 = D(0)/S(0) = D(0)/3F(0)_m$, or

$$r_0 = -\frac{\displaystyle\int I(\mathbf{r})\rho(\mathbf{r}, \hat{\mu}, 0) P_2\,(\hat{\mu} \cdot \hat{z})\mathrm{d}^3\mathbf{r}\mathrm{d}^2\hat{\mu}}{\displaystyle\int I(\mathbf{r})[n_0 - n(\mathbf{r}, 0)]\mathrm{d}^3\mathbf{r}}. \tag{16}$$

To evaluate r_0, we examine the photobleaching reaction. For convenience we assume the bleach pulse has intensity $I_b(\mathbf{r})$ at each position $\mathbf{r}$ that is constant over a period T, which is sufficiently brief to neglect label motion. We pick positions such that the maximum bleach intensity occurs at $\mathbf{r} = 0$ and define $f(\mathbf{r}) = I_b(\mathbf{r})/I_b(0)$. Because the bleach and observation profiles are identical, $f(\mathbf{r})$ is also equal to $I(\mathbf{r})/I(0)$. We assume that photobleaching is an irreversible first-order reaction, with the rate of inactivation of a label at position $\mathbf{r}$ being $3q_b I_b(0) f(\mathbf{r})(\hat{\mu} \cdot \hat{z})^2$, where q_b is an inactivation coefficient for the label. The degree of bleaching achieved by the pulse is then characterized by a parameter K, where $K = q_b T I_b(0)$.

The most useful results occur for small bleaching pulses for which $K \ll 1$. In this case, we obtain the initial distribution

$$\rho(\mathbf{r}, \hat{\mu}, 0) = (n_0/4\pi)[1 - 3Kf(\mathbf{r})(\hat{\mu} \cdot \hat{z})^2], \tag{17}$$

and r_0 reduces to $\frac{2}{5}$, regardless of the bleaching pattern used.

At higher K values, the general solution

$$\rho(\mathbf{r}, \hat{\mu}, 0) = (n_0/4\pi) \exp[-3Kf(\mathbf{r})(\hat{\mu} \cdot \hat{z})^2], \tag{18}$$

must be used and the results will depend on the particular bleaching pattern. Stronger bleaches cause r_0 to decrease

from ⅔ and approach zero as $K \gg 1$. Expanding Eq. 18 to order K^2 gives $r_0 = 0.4[1 - (27/70)gK]$, where

$$g = \int f(\mathbf{r})^3 d^3\mathbf{r} / \int f(\mathbf{r})^2 d^3\mathbf{r}, \tag{19}$$

such that $g = 1$ for a uniform optical pattern and ⅔ for a Gaussian beam.

Any rotational motion during the bleaching period will produce apparent r_0 values that are reduced from these calculated values. At small K values, this motion can be accounted for by treating a particular $r(t)$ model as an impulse response function to be convoluted with the bleaching pulse. At large K values, convolution techniques cannot be used and one would have to solve diffusion equations with an orientationally dependent photobleaching sink term.

In practice some degree of restricted wobble motion of the label about its attachment site would always be expected. This motion generally relaxes in several nanoseconds or less, whereas typical bleaching periods last microseconds and longer. Rapid, unresolvable wobbling motion can be qualitatively incorporated into $r(t)$ by assuming that each label dipole is uniformly distributed within a cone of semiangle α about some unit vector $\hat{\mu}^*$ that is fixed during the bleaching period. For $K \ll 1$, we evaluate Eq. 16 and find the apparent initial anisotropy

$$r_0 = 0.1[\cos \alpha(1 + \cos \alpha)]^2, \tag{20}$$

from which angle α can be obtained. As expected, r_0 becomes vanishingly small if the label wobbles over a large angular region. The observed decay of the anisotropy from this initial value then involves the much slower motions of $\hat{\mu}^*$. Evaluating Eq. 11 for $K \ll 1$, we find

$$r(t) = r_0 \langle P_2[\hat{\mu}^*(t) \cdot \hat{\mu}^*(0)] \rangle \tag{21}$$

where r_0 is given by Eq. 20 and $\langle P_2[\hat{\mu}^*(t) \cdot \hat{\mu}^*(0)] \rangle$ as given by Eq. 12 involves the dot product between a label's $\hat{\mu}^*$ vector at times t and 0. Generalizations for large K values can also be made, although we shall not do so here.

Fluorescence Recovery at the Magic Angle

To obtain a dynamic expression for $\Delta F(t)_m$, we combine Eqs. 4 and 10b:

$$\Delta F(t)_m = q \iint I(\mathbf{r}) W(\mathbf{r}, \mathbf{r}', t)[n_0 - n(\mathbf{r}', 0)] d^3\mathbf{r} d^3\mathbf{r}'. \tag{22}$$

Eq. 22 cannot be immediately factored like $r(t)$ into one term that depends on the initial bleach pattern multiplied by another term that contains translational diffusion dynamics. This is true even though $W(\mathbf{r}, \mathbf{r}', t)$ depends only on the distance Δr between $\mathbf{r}$ and $\mathbf{r}'$, i.e.,

$$W(\mathbf{r}, \mathbf{r}', t) = (4\pi D_t t)^{-3/2} \exp(-\Delta r^2/4D_t t), \tag{23}$$

where D_t denotes the particle's translational diffusion coefficient.

In our setup, the focused laser beam has a Gaussian profile that passes through thin curvettes with a constant waist w. Thus $f(\mathbf{r})$ is cylindrically symmetric about the y-axis and independent of the y-coordinate. From Axelrod et al. (1976), an initial concentration distribution of the form

$$n(\mathbf{r}, 0)/n_0 = 1 + \sum_{m=1}^{\infty} A_m[-Kf(\mathbf{r})]^m/m!, \tag{24}$$

yields the series solution

$$F(t)_m/F_0 = -\sum_{n=1}^{\infty} A_n[(-K)^n/n!]/[1 + n(1 + 2t/\tau)], \tag{25}$$

where $\tau = w^2/4D_t$.

For an instantaneous bleaching pulse at $t = 0$, Eq. 18 gives

$$n(\mathbf{r}, 0)/n_0 = \int_0^1 \exp[-3Kf(\mathbf{r})s^2] ds, \tag{26}$$

where s is a dummy variable. From this, $A_m = 3^m/(2m + 1)$, which differs from the $A_m = 1$ value of Axelrod et al. (1976). They used the initial distribution

$$n(\mathbf{r}, 0)/n_0 = \exp[-Kf(\mathbf{r})], \tag{27}$$

which corresponds to the assumption that each label freely rotates over all angles during the bleach period, rather than remaining at a fixed direction. These two results constitute static and dynamic limits of rotational mobility.

To qualitatively evaluate intermediate cases of restricted rotational motion during the bleaching period, we use the wobble model. We treat a rapidly moving label as if its dipole were uniformly distributed within a cone of semiangle α that is fixed during the bleaching period. This gives

$$n(\mathbf{r}, 0)/n_0 = \int_0^1 \exp[-Kf(\mathbf{r})[1 + 2XP_2(s)]] ds, \tag{28}$$

where $X = 0.5 \cos \alpha(1 + \cos \alpha)$, which yields

$$A_m = \int_0^1 [1 + 2XP_2(s)]^m ds \tag{29a}$$

or

$$A_m = \sum_{n=0}^{m} 3^n m! X^n (1 - X)^{m-n}/[(2n + 1)n!(m - n)!]. \tag{29b}$$

As $\alpha \to 0$, we regain the static limit values $A_m = 3^m/(2m + 1)$, whereas either $\alpha = 90°$ or $180°$ gives the dynamic limit values $A_m = 1$. For other values of α, A_m lies between these values.

At small values of K, the degree of label rotational mobility during the bleach is immaterial as far as $\Delta F(t)_m$ is concerned. To first order in K, Eq. 28 becomes $n(\mathbf{r}, 0)/n_0 = 1 - Kf(\mathbf{r})$ regardless of α, Eq. 25 reduces to

$$\Delta F(t)_m/F_0 = 0.5K/(1 + t/\tau), \tag{30}$$

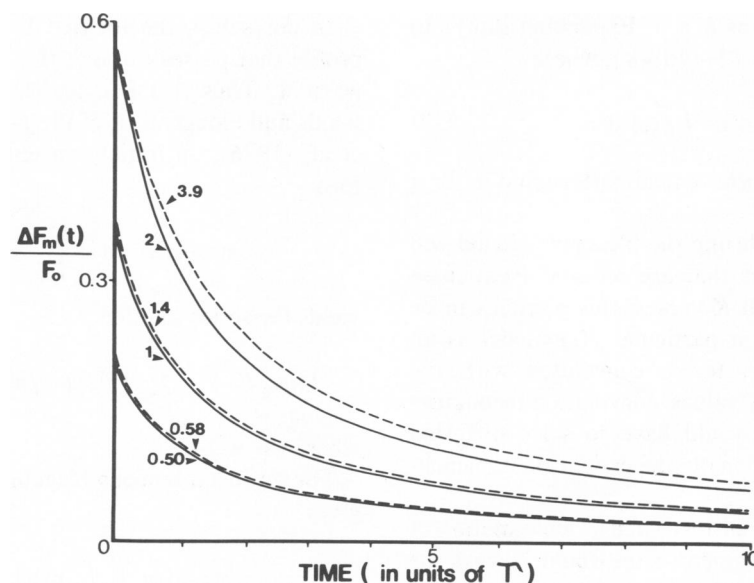and K can be uniquely determined as $K = 2\Delta F(0)_m/F_0$.

FIGURE 2 Fluorescence photobleaching recovery curves at the magic angle for a freely diffusing single species and a Gaussian profile laser beam are presented. $\Delta F(t)_m/F_0$ given by Eq. 25 is plotted against time in units of τ. The dashed curves indicate the absorption dipole is fixed during the bleach and the solid curves indicate the dipole rotates rapidly and uniformly over all angles during the bleach. The number by each curve shows the value of the bleaching parameter K used. K values were chosen such that pairs of solid and dashed curves start from the same $\Delta F(0)_m/F_0$.

At larger K values, differences in label rotational mobility will affect the initial value and shape of the $\Delta F(t)_m$ curves as the initial concentrations weight the translational diffusion modes differently. In the dynamic and static limits, $\Delta F(0)_m/F_0$ is respectively found to be 0.115 and 0.109 for $K = 0.25$; 0.213 and 0.191 for $K = 0.5$; 0.368 and 0.308 for $K = 1.0$; 0.568 and 0.443 for $K = 2$; 0.755 and 0.572 for $K = 4$; and so forth. In Fig. 2 we compare curve shapes for several pairs of dynamic and static cases whose K values are chosen such that their $\Delta F(0)_m/F_0$ values match. As seen, the static case always recovers more slowly than the dynamic case. For K values in the dynamic cases up to at least 2, the percentage difference between curve pairs is found to be $\sim 1.4~Kt/\tau\%$ for $t < 5\tau$, with little further increase after 5τ. Using a late recovery time $t = 15\tau$ and K values for the dynamic cases, we find differences of 1.7% for $K = 0.25$, 4% for $K = 0.5$, 8% for $K = 1.0$, and 17% for $K = 2.0$. These results show that $\Delta F(t)_m$ is insensitive to a label's rotational motion during the bleach pulse for K values sufficiently below unity.

CONCLUSION

The FPR design analyzed here offers several advantages for solution studies. The magic angle measurement in the small bleaching regime is obviously desirable when trying to extract information concerning translational motions because the recovery curves are independent of label rotational mobility both during and following the bleaching period. This may be helpful in complex situations such as those seen in the recent studies of actin polymerization (Lanni et al., 1981) and the binding of ethidium bromide to

DNA (Icenogle and Elson, 1983a,b). Additional information about rotational motions can also be obtained by a combination of parallel and perpendicular measurements. As a tool for rotational studies, FPR offers the possibility of studying extremely slow relaxations that are beyond the time scales accessible to current techniques involving triplet-state lifetimes. In fact, Smith et al. (1981) have previously applied FPR to oriented membrane systems using lipid labels with rotational relaxation times of several minutes. Although designs such as theirs could also be applied to solution studies, the variant described here leads to simplified equations, allows the orientational and non-orientational contributions to the fluorescence recovery signal to be cleanly separated, and eliminates uncertainties about the relative orientation between a label's absorption and emission dipoles.

REFERENCES

Aragon, S. R., and R. Pecora. 1975. Fluorescence correlation spectroscopy and Brownian rotational diffusion. Biopolymers. 14:119–138.

Aragon, S. R., and R. Pecora. 1976. Fluorescence correlation spectroscopy as a probe of molecular dynamics. J. Chem. Phys. 64:1791–1803.

Axelrod, D., D. E. Koppel, J. Schlessinger, E. Elson, and W. W. Webb. 1976. Mobility measured by analysis of fluorescence photobleaching recovery kinetics. Biophys. J. 16:1055–1069.

Ehrenberg, M., and R. Rigler. 1972. Polarized fluorescence and rotational Brownian motion. *Chem. Phys. Lett.* 14:539–544.

Ehrenberg, M., and R. Rigler. 1974. Rotational Brownian motion and fluorescence intensity fluctuations. *Chem. Phys.* 4:390–401.

Ehrenberg, M., and R. Rigler. 1976. Fluorescence correlation spectroscopy applied to rotational diffusion of macromolecules. *Q. Rev. Biophys.* 9:69–79.

Icenogle, R. D., and E. L. Elson. 1983*a*. Fluorescence correlation spectroscopy and fluorescence photobleaching recovery of multiple binding reactions. I. Theory and FCS measurements. *Biopolymers.* 22:1919–1948.

Icenogle, R. D., and E. L. Elson. 1983*b*. Fluorescence correlation spectroscopy and fluorescence photobleaching recovery of multiple binding reactions. II. FPR and FCS measurements at low and high DNA concentrations. *Biopolymers.* 22:1949–1968.

Kinosita, K., Jr, S. Kawato, and A. Ikegami. 1977. A theory of fluorescence polarization decay in membranes. *Biophys. J.* 20:289–305.

Lanni, F., D. L. Taylor, and B. R. Ware. 1981. Fluorescence photobleaching recovery in solutions of labeled actin. *Biophys. J.* 35:351–364.

Smith, L. M., R. M. Weis, and H. M. McConnell. 1981. Measurement of rotational motion in membranes using fluorescence recovery after photobleaching. *Biophys. J.* 36:73–91.

Perrin, F. 1934. Mouvement Brownien d'un ellipsoide (I). Dispersion dielectrique pour des molecules ellipsoidales. *J. Phys. Radium.* 5:497–511.

Rigler, R., and P. Graselli. 1980. Time-resolved fluorescence spectroscopy and diffusion of biological molecules. *In* Lasers in Biology and Medicine. F. Hillenkamp, R. Prater, and C. A. Sacchi, editors. Plenum Publishing Co., New York. 151–163.

Rigler, R., P. Graselli, and M. Ehrenberg. 1979. Fluorescence correlation spectroscopy and application to the study of Brownian-motion of biopolymers. *Physica Scripta.* 19:486–490.

Wahl, Ph. 1975. Decay of fluorescence anisotropy. *In* Biochemical Fluorescence Concepts, Vol. 1. R. F. Chen and H. Edelhoch, editors. Marcel Dekker, Inc., New York. 1–41.

Wegener, W. A. 1984. Fluorescence recovery spectroscopy as a probe of slow rotational motions. *Biophys. J.* 46:795–803.